Nanoscale Res Lett (2009) 4:1183–1190
DOI 10.1007/s11671-009-9381-z

NANO EXPRESS

The Modulation of Optical Property and its Correlation with Microstructures of ZnO Nanowires

Haohua Li · Chaolun Liang · Kuan Zhong · Meng Liu · Greg A. Hope · Yexiang Tong · Peng Liu

Received: 20 April 2009 / Accepted: 15 June 2009 / Published online: 1 July 2009

Abstract ZnO nanowires with both good crystallinity and oxygen vacancies defects were synthesized by thermal oxidation of Zn substrate pretreated in concentrated sulfuric acid under the air atmosphere, Ar- and air-mixed gas stream. The photoluminescence spectra reveal that only near-band-edge (NBE) emission peak was observed for the sample grown in the air atmosphere; the broad blue–green and the red-shifted NBE emission peaks were observed for the sample grown in the mixed gas stream, indicating that the sample grown in the mixed gas stream has a defective structure and its optical properties can be modulated by controlling its structure. The high-resolution transmission electron microscope and the corresponding structural simulation confirm that the oxygen vacancies exist in the crystal of the nanowires grown in the mixed gas stream. The ZnO nanowires with oxygen vacancies defects exhibit better photocatalytic activity than the nanowires with good crystallinity. The photocatalytic process obeys the rules of first-order kinetic reaction, and the rate constants were calculated.

Keywords ZnO nanowires · Thermal oxidation · Oxygen vacancies · Photoluminescence · Photocatalysis

H. Li · K. Zhong · M. Liu · Y. Tong (✉) · P. Liu (✉)
School of Chemistry and Chemical Engineering, Sun Yat-Sen University, 510275 Guangzhou, People's Republic of China
e-mail: chedhx@mail.sysu.edu.cn

P. Liu
e-mail: pengliupd@hotmail.com

H. Li
e-mail: lihaohua@mail2.sysu.edu.cn

H. Li · K. Zhong · M. Liu · Y. Tong · P. Liu
MOE of Key Laboratory of Bioinorganic and Synthetic Chemistry, Sun Yat-Sen University, 510275 Guangzhou, People's Republic of China

H. Li · K. Zhong · M. Liu · Y. Tong · P. Liu
Institute of Optoelectronic and Functional Composite Materials, Sun Yat-Sen University, 510275 Guangzhou, People's Republic of China

C. Liang
Instrumental Analysis & Research Center, Sun Yat-Sen University, 510275 Guangzhou, People's Republic of China

G. A. Hope
School of Science, Griffith University, Nathan, QLD 4111, Australia

Introduction

Nanostructured ZnO has been the source of great scientific interest, toward both the understanding and exploitation of its intrinsic properties and the performance in optoelectronic applications due to its direct wide band gap of 3.35 eV at 300 K and the high exciton binding energy of 60 meV [1]. Consequently, fabricating ZnO nanostructures with different sizes and morphologies is of great importance for fundamental research and the development of novel devices. To date, various ZnO nanostructures have been successfully synthesized, including quantum dots, nanorods, nanowires, nanobelts, nanorings, nanocups, nanodisks, nanoflowers, nanonails, nanospheres, and hierarchical nanostructures [2–8]. Among them, ZnO nanowires have attracted intensive research interest and have been emerging as promising candidates for short-band semiconductor laser devices and visible photoelectronics devices such as room temperature lasers, light-emitting diodes, ultraviolet (UV) detectors, field-emission displays, photonic crystals, and solar cells [1, 9].

However, various defects often exist in ZnO nanowires and these defects can affect the electrical and optical properties [10]. For example, ZnO nanowires with oxygen vacancies exhibit photocatalytic activity [11]. So far, there is still controversy of whether the oxygen vacancies or other native defects affect the properties of ZnO nanowires [12–14]. As for the photoluminescence (PL) property of ZnO nanowires, two PL peaks can be observed, one in the range of UV region, the other in the visible region (usually broad blue–green peaks). The UV emission originated from the excitonic recombination corresponding to the near-band-edge (NBE) emission [4], the visible luminescence, is generally referred to deep level (DL) emission; it is now quite generally accepted that the blue–green luminescence in ZnO arises from a radiative recombination involving an intrinsic defect, which is believed to be due to one or more of the following native defects: zinc vacancy (V_{Zn}), oxygen vacancy (V_O), zinc interstitial (Zn_i), oxygen interstitial (O_i), or antisite oxygen (O_{Zn}) [11, 15–17]. However, there is no satisfactory consensus due to the complexity of the detailed microstructure of ZnO. Different hypotheses were proposed to explain the origin of DL emission; the commonly cited reason is that the recombination of a photogenerated hole with an electron occupying the oxygen vacancy [18]. It proved that high-resolution transmission electron microscopy (HRTEM) with structure simulation is a powerful technique for investigating microstructure of nanowires, so do the defects in ZnO nanowires. However, to our best knowledge, previous studies did not associate HRTEM results with PL properties, which can provide favorable evidence of microstructure for origin of DL emission.

To date, there have been considerable efforts directed at the vapor-based routes to prepare and fabricate ZnO nanowires such as chemical vapor deposition [19, 20], thermal evaporation [21–24], vapor–liquid–solid (VLS) growth [25], and thermal oxidation [26–33]. The parameters of fabrication such as composition of the source materials, vacuum pressure, and growth ambient, reaction temperature, substrate could drastically influence the morphology and properties of grown ZnO nanowires. However, the fabrication of ZnO nanowires with large volume of oxygen vacancies often confronts the problems of tedious operation procedures [9, 20, 21, 24, 26, 30].

Here we report the facile and controllable growth of ZnO nanowires with large volume of oxygen vacancies by thermal oxidation of the zinc substrate, which had been treated in concentrated sulfuric acid under different oxygen-containing atmospheres. Porous ZnO film was formed on zinc substrate by being passivated in concentrated sulfuric acid. The porous ZnO film can be used as a "hard template" to confine the growth of ZnO nanowires along one dimension. The relation between PL properties and crystal defects of ZnO nanowires was discussed. Furthermore, the correlation of the oxygen content with the crystal defects of the nanowire was investigated by HRTEM and its structure simulation. In addition, the difference in photocatalytic properties owing to crystal defects was observed. These results support that the blue light emission of ZnO nanowires originates from oxygen vacancies and that its optical properties can be modulated by controlling the oxygen vacancies.

Experimental

Synthesis of ZnO Nanowires

A zinc foil (99.98%) was used as the substrate for the growth of ZnO nanowires. After being polished and washed by dilute hydrochloric acid and de-ionized water, the zinc foil was put into concentrated sulfuric acid (98%) and passivated for 6 h to form a porous oxide film. The annealing temperature was increased to 500 °C at a rate of 10 °C/min and held at this higher temperature for 5 h and cooled down naturally. Two different atmospheres were chosen: the air atmosphere and the mixed gas stream (5% air, 95% Ar) at a total flow rate of 80 standard cubic centimeters per minute (sccm); the dark gray compacted thin film and white powder were obtained at the corresponding atmosphere.

Structural Characterization

The morphology of all the samples was observed by a field-emission scanning electron microscope (FE-SEM, JSM 6330F, JEOL). The crystal structure was determined by a transmission electron microscope (TEM, JEM 2010HR, JEOL) with an Oxford Energy dispersive X-ray spectrometer (EDS) and the X-ray diffractometer (XRD, PW 1830, Philips).

Optical Characterization

The dispersion solutions containing ZnO nanowires of different sizes were obtained as follows [34]. White powders (ZnO nanowires grown in the mixed gas stream) were dispersed in dimethylformamide (DMF, spectrum grade), sonicated for 1 h, and the sediment was collected after 8 h subsidence. The remaining dispersion system was resonicated for 1 h, subsided for 30 h, and then the sediment was separated from the solution. Finally, this procedure was repeated, but the sediment was obtained after 60 h subsidence. The last remaining dispersion was named as residual dispersion, and the sediments were sequently marked as sediment-1,-2 and -3. The dark gray compacted thin film (grown in air atmosphere) was also dispersed in DMF,

which is different from white powder in that it was only sonicated for 1 h, and subsided for 15 h, and then the sediment was obtained after 15 h subsidence. These sediments were dispersed in DMF again, sonicated for 15 min, and the PL measurement was performed at room temperature using the 325 nm line of Xe lamp (PL, RF-5301, Shimadzu).

Photocatalytic activity experiments: The quartz reactor was an orbicular tube filled with 160 mL 15 mg/L methyl orange (MO) aqueous solution and 60 mg ZnO nanowires. The UV lamp (6 W) was placed in the center of the tube and surrounded by the reactor. Prior to irradiation, the solution was sonicated for 30 min and then stirred in the dark for 30 min to establish absorption–desorption equilibrium. The reactive mixture was stirred under UV irradiation. The mixture was sampled at different times and centrifuged for 5 min to discard any sediment. The analysis of the solution was performed with a UV–Vis spectrophotometer (UV–Vis UV-2501PC, Shimadzu).

Results and Discussion

Figure 1 presents the XRD pattern of the sample. The diffraction peaks (100), (002), (101), (102), (110), (103), and (112) are exactly indexed to the hexagonal ZnO phase (JCPDS 65-3411). The peaks (101) and (201) were caused by the Zn substrate. EDS analysis showed that only zinc and oxygen elements were found, indicating that the product is pure.

Figure 2 shows the typical FE-SEM image of the ZnO nanowires. Figure 2a depicts the morphology of the nanowires grown at 500 °C for 5 h in the air atmosphere.

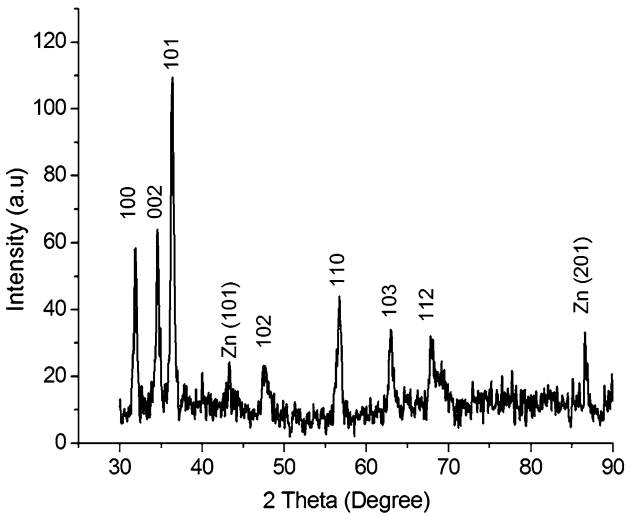

Fig. 1 XRD pattern of the sample obtained by thermal oxidation, 500 °C, 5 h, the air atmosphere

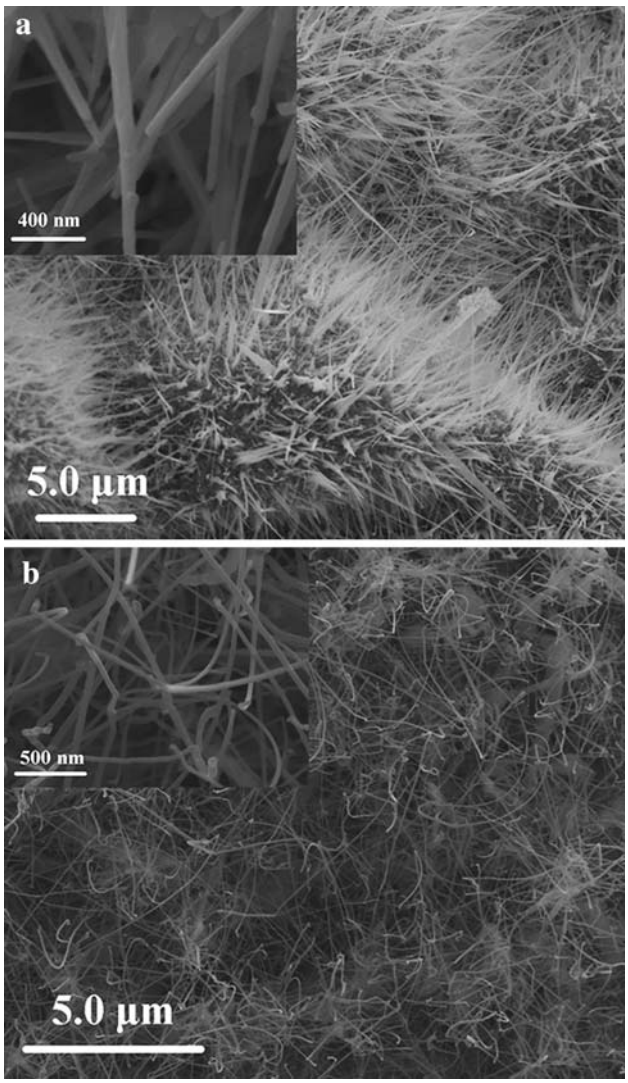

Fig. 2 Typical low- and high-magnification (*inset*) SEM images of ZnO nanowires grown at 500 °C in different atmosphere for 5 h. **a** Air atmosphere; **b** the mixed gas stream

The surface of the annealed sample was compactly covered with dense ZnO nanowires. The prepared ZnO nanowires are straight with a sharp tip. However, it can also be seen that the diameter of the single ZnO nanowires is not uniform, from root to tip and that the diameter is successively increased in the nanosize dimension. The length of ZnO nanowires varies from several micrometers to over ten micrometers. The diameter of the nanowires ranges from 20 to 80 nm, the average diameter being 50 nm (from inset in the Fig. 2a).

Figure 2b depicts the typical morphology of the nanowires grown at 500 °C for 5 h in the mixed gas stream. As shown in the Fig. 2b, the white powder consists of a large quantity of entangled and curved nanowires. Otherwise, the length of ZnO nanowires is so long, which is over several ten micrometers and the diameter of ZnO nanowires is

about 30 nm, which is quite different from the nanowires grown in the air atmosphere by comparing with Fig. 2a, b. On the other hand, the oxygen content can also affects the shape of the nanowires.

In our experiments, we found that only a few and short nanowires can grow on the untreated Zn substrate. The SEM image showed that porous ZnO film formed on the surface of Zn substrate after being treated in concentrated sulfuric acid [35]. Thus, the Zn atoms in the holes were oxidized, and ZnO nanowires grew from the holes, which can be used as a "hard template".

Figure 3 shows the room-temperature PL spectra of the ZnO nanowires excited at 325 nm. Figure 3a is the PL spectra of the nanowires grown in the air atmosphere and Fig. 3b is the PL spectra of the samples grown in the mixed gas stream.

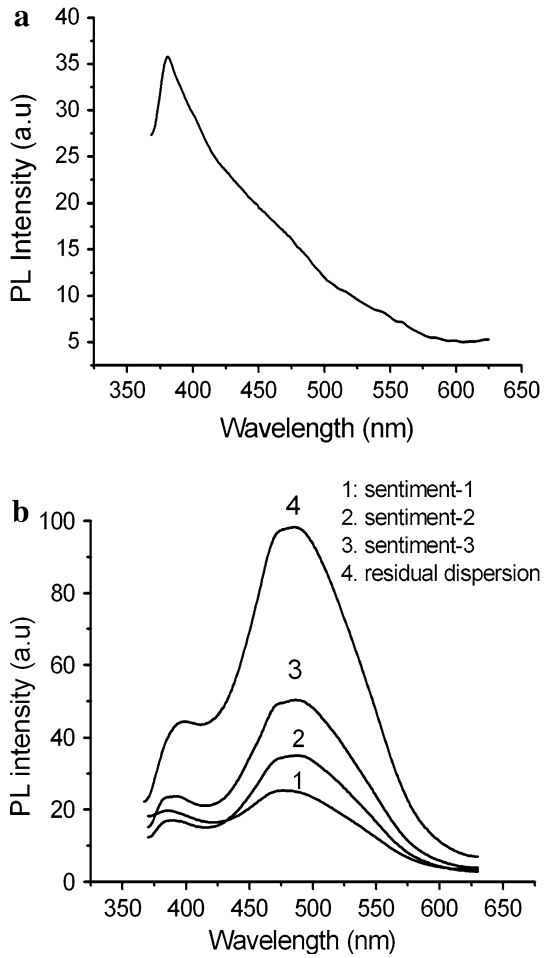

Fig. 3 The room-temperature PL spectra of ZnO nanowires. **a** Grown in air atmosphere; **b** grown in the mixed gas stream. The samples were dispersed in DMF, sonicated for 1 h, and the sediment-1 was collected after 8 h subsidence. The remaining dispersion system was resonicated for 1 h, subsided for 30 h, and then the sediment-2 was separated. This procedure was repeated, the sediment-3 was obtained after 60 h subsidence. The last remaining dispersion was named as residual dispersion. These sediments were dispersed in DMF again, sonicated for 15 min, and the PL measurement was performed at room temperature

From Fig. 3a, it can be observed that the spectra show strong and sharp UV emission peak positioned at 381 nm. It had been demonstrated that the optical properties of semiconductor materials are related to both intrinsic and extrinsic effects. Intrinsic optical effects via the transition take place between the electrons in the conduction band and holes in the valence band, including excitonic effects. Excitons are classified into free excitons [FX] and bound excitons [BX]. Extrinsic effects are related to dopants or native defects. Generally, excitons are prone to bound to donors and acceptors [36]. So the UV emission peak at room temperature is well understood as NBE emission caused by FX and BX recombination, etc., which can be distinguished in low-temperature PL spectra [37–40]. Otherwise, a variety of DL defects, such as oxygen, zinc vacancies, and interstitials have been proposed as possible contributors to the visible emission. Thus, no DL emission peaks were found in Fig. 3a. It can be demonstrated that the nanowires grown in air atmosphere should have good crystallinity.

From Fig. 3b, it can be seen that the spectra show very weak UV emission peaks and strong broad blue–green emission peaks, and with the decrease in the nanowires diameter, the red-shift of the UV emission peaks (386, 389, 392, and 399 nm) were observed, while the blue–green peaks almost have the same position at 486 nm around. As mentioned above, the blue–green emission peaks originated from the intrinsic defects in undoped ZnO nanowires and the possible defects included V_{Zn}, V_O, Zn_i, O_i, and O_{Zn}. These defects, especially V_{Zn} [41] and V_O [42], have been proposed as carriers of the blue–green emission, but different opinions on the effect of these factors still exist. The question arises as to what kind of defect is the origin of the broad blue–green peak. It can be noticed that the origin of broad blue–green peak is related to annealing atmosphere because there is no DL emission peak in Fig. 3a. Compared with the air atmosphere, the mixed gas stream is oxygen deficient. Thus, the origin of broadblue–green peak is likely to be V_O and Zn_i which are prone to be formed in oxygen-deficient condition [17]. However, it was reported that the DL emission of Zn_i and V_O was located in red ($\sim$600 nm) and green ($\sim$500 nm) regions, respectively [43]. Therefore, we can conclude that the blue–green emission peaks were caused by the defects of oxygen vacancies. Thus, in this work, the UV emission is ascribed to ultraviolet excitonic recombination of the NBE transition, and the broad blue–green band emission (DL emission) can be explained as the radial recombination of photo-generated hole with the electron occupying the oxygen vacancy [18].

On the other hand, as for the Einstein shift of the UV emission peaks with the decrease in the nanowires diameter, it is determined by two contrary factors: BX recombination and quantum confinement effect caused by FX recombination [44]. It was reported that increasing the amount of BX can result in the red-shift of the NBE peak position [44]. However, in this case, the quantum confinement effect can be ruled out. Because the Bohr radius of ZnO is only about 2 nm [45], it is not likely that the ZnO nanowires with diameter of 30 nm will change the band gap due to quantum confinement. Therefore, red-shift of the NBE peak position can be ascribed to bound exciton emission. And by decreasing the diameter, the ratio of surface area to volume increased, which can favor a high level of surface and sub-surface oxygen vacancies [46]. Thus, in this case, the amount of BX increased with the increase in oxygen vacancies and the UV emission shifted to longer wavelength.

To sum up, the following phenomena were observed in the PL experiment: (1) the blue–green emission peaks were not observed for the samples grown in the air atmosphere; (2) the peak position of the UV emission shifted to longer wavelength with the decrease in ZnO nanowires diameter for the samples grown in Ar- and air-mixed atmosphere. All these phenomena are in good agreement with each other and can be reasonably attributed to the defects of oxygen vacancies of ZnO nanowires.

To verify the crystal structure of ZnO nanowires grown at different atmospheres, the HRTEM experiments were carried out. Figure 4a shows a typical TEM image of the samples grown in the air atmosphere. A fragment of ZnO nanowire was captured, whose diameter is about 30 nm. The inset in Fig. 4a shows the select-area electron diffraction (SAED) pattern taken along [010] zone axis. Sharp and clear diffraction spots were observed, which indicates that ZnO nanowires have a quite good single-crystalline structure. The reflections correspond to (0001), (0002), (10$\bar{1}$0) lattice planes of ZnO with hexagonal structure indexed, which is in good agreement with XRD results. In addition, the growth direction of ZnO nanowire is along (0001) facet. The high-resolution TEM (HRTEM) image of the circled area in Fig. 4a is shown in Fig. 4b. The clear lattice fringe between (0001) crystal planes and (10$\bar{1}$0) crystal planes with d spacing of 0.52 and 0.28 nm, respectively, can be observed. No obvious crystalline defects in the ZnO nanowire were found in the HRTEM image, indicating a good quality of crystalline structure. The HRTEM image confirms the results obtained from SAED.

Figure 5a shows the TEM image of a ZnO nanowire from the sample grown in Ar and air mixed gas stream. The diameter of ZnO nanowire is about 40 nm. The SAED patterns of the circled area in Fig. 5a were taken along [010] zone axis. The sharp diffraction spots indicate that

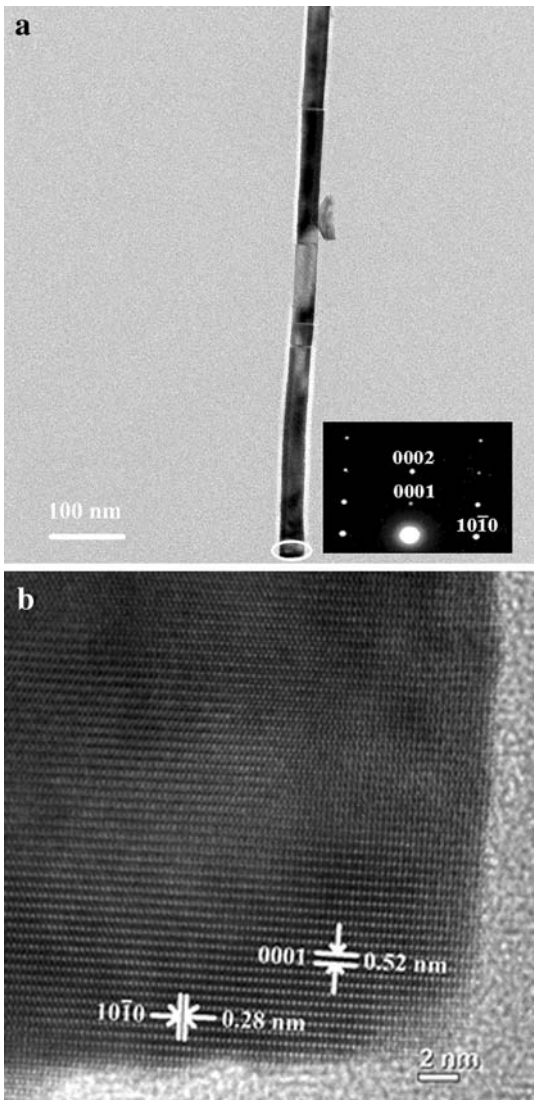

Fig. 4 **a** TEM image of ZnO nanowire annealed at 500 °C in the air atmosphere for 5 h, *inset* shows the SAED pattern of *circled area*; **b** HRTEM image of *circled area*

the nanowire is single crystalline. The pattern can be indexed as (10$\bar{1}$0), (10$\bar{1}$0) and (0001) lattice planes of ZnO with hexagonal structure. The growth direction of ZnO nanowire is along (10$\bar{1}$0) facet. However, it should be noticed that the streaks appeared in the SAED pattern along (0001) facet, as indicated by white arrowheads in SAED pattern. These streaks may be caused by the sharp edge of the nanowires or the planar defects along (0001) direction [47].

Figure 5b presents the HRTEM image of circled area in Fig. 5a. It can be found that the growth facets of the ZnO nanowire were (10$\bar{1}$0) and (0001), and the growth direction is along (10$\bar{1}$0) facet. It clearly shows that there are several sharp-contrast lines, indicating different crystallinity from the surrounding area, which are caused by the variation in

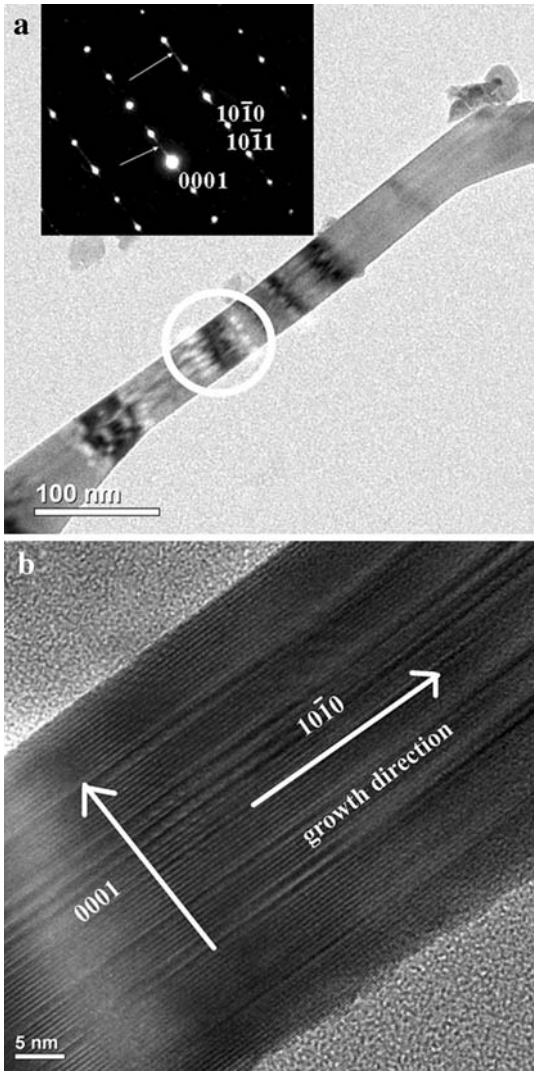

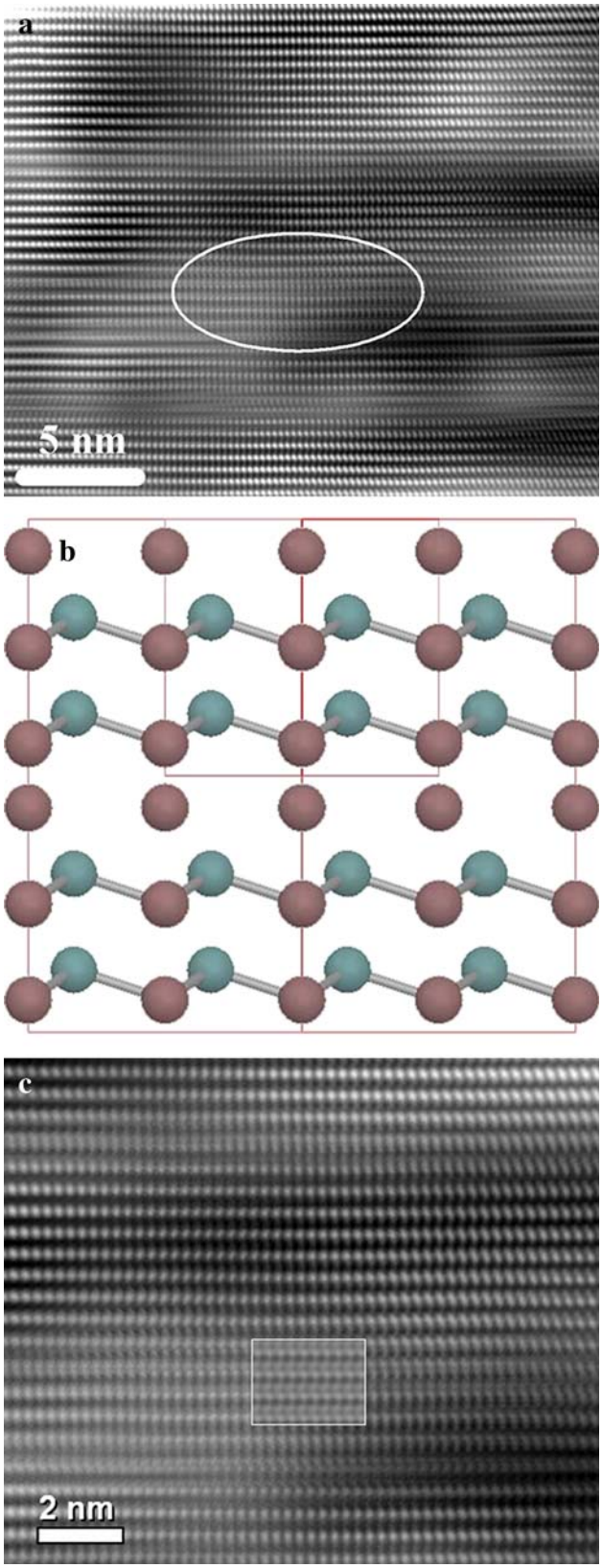

Fig. 5 **a** TEM image of ZnO nanowire annealed at 500 °C for 5 h in Ar and air mixed gas stream for 5 h, *inset* shows the SAED pattern of the *circled area* in Fig. 5a; **b** HRTEM image of *circled area* in Fig. 5a

the interplanar spacing along the vertical direction corresponding to planar defects. The question arises as to what kind of planar defect exists in the nanowires. It cannot be interstitial layer introduced by impurities, because no other elements were included in the system except atomic Zn and O and EDS analysis confirmed this deduction.

In order to ascertain the defects, HRTEM simulation was carried out by using Jems2.1 software. Figure 6a shows the experimental HRTEM image. The contrast difference in the circled area shows the existence of some planar defects, which might arise from the existence of oxygen vacancies. A structural model of hexagonal ZnO is shown in Fig. 6b, in which the structure is constituted by packing of Zn atoms (red) and O atoms (blue) layer by layer in hexagonal sequence by taking off some oxygen atoms along 0001 direction as indicated by arrowhead. It can be seen that the HRTEM image (Fig. 6c) matches the simulation image (inset in Fig. 6c) very well. Therefore, it

◀ **Fig. 6** **a** HRTEM images of ZnO nanowire annealed in the mixed gas stream (Ar and air); **b** The defective structural model of hexagonal ZnO where the oxygen ions are taking off as shown by *arrowheads*. The simulation was for 200 kV electrons, Cs = 1.6 nm, the defocus is −107 nm and the thickness is 1.9 nm; **c** Enlarged HRTEM image and the *inset* obtained by the simulation

can be concluded that the planar defect was caused by oxygen vacancies. The structure characterization is in closely accord with the deduction from PL spectra. The nanowires grown in the mixed gas stream have intrinsic defects, which are ascertained as O vacancies, and the nanowires grown in the air atmosphere have a good crystallinity. The above results reveal that ZnO nanowires with different structures or defects will show different PL performance. Therefore, it is possible to modulate their optical properties by varying their structures or intrinsic defects structure through different synthesizing methods.

It has been well reported that ZnO is an important photocatalyst. Therefore, methyl orange (MO) was employed to investigate the photocatalytic degradation of the organic dyes by the ZnO nanowires grown in different atmospheres. Figure 7 presents the degradation rate curves of MO, where c is the residual concentration of MO after irradiation and c_0 is the initial concentration before irradiation. It can be seen that the degradation rate significantly decreased to 12.8% after UV irradiation for 30 min and 2% on prolonging the irradiation time to 60 min for catalyst of ZnO nanowires grown in the mixed gas stream. However, it needed the irradiation time of 30 min to decompose the MO to 26.5% for nanowires grown in the air atmosphere. On the other hand, the plots of $\ln(c/c_0)$ versus time suggest that the photodecomposition reaction follows the first-order rate law. The calculated rate constant is 1.0×10^{-3} s^{-1} with the photocatalyst of ZnO nanowires grown in the mixed gas stream, 8.2×10^{-4} s^{-1} with ZnO nanowires. So, the photocatalytic activity of ZnO nanowires (grown in the mixed gas stream) is higher than that of the ZnO

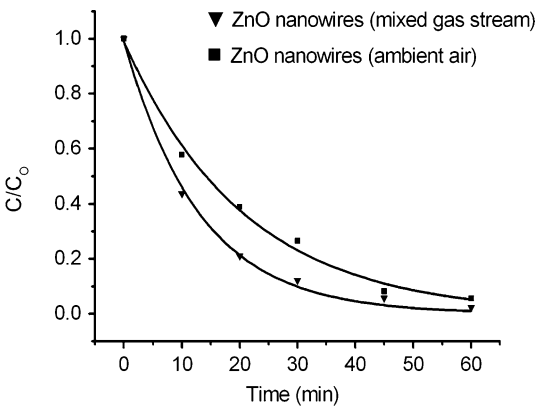

Fig. 7 Curves of the degradation rate of MO and UV irradiation time with the photocatalyst of the ZnO nanowires grown in different atmospheres

nanowires (grown in air atmosphere). The photocatalytic process of ZnO can be interpreted by energy band theory of semiconductor [11]. When the photo energy of UV light exceeds or is equal to the band gap of ZnO crystal, some electrons in the valence band (VB) can be excited to the conduction band (CB) to form the photo-generated electrons in the CB and the same amount of holes in the VB. The holes in the VB are prone to react with surface hydroxyl groups and H_2O to form hydroxyl radicals (·OH), which can partly or completely mineralize the organic chemicals. In the meanwhile, photo-generated electrons in the VB can easily react with the O_2 to form $\cdot O_2$ radical groups. In this experiment, the ZnO nanowires grown in the mixed gas stream contain large amounts of O vacancies, which can be recognized as electron donor. These donors can produce some excess electrons in the CB and some additional holes in the VB, which can generate more radical and further improve the photocatalytic property. Therefore, ZnO nanowires grown in the mixed gas stream exhibit better activity than ZnO nanowires grown in air atmosphere.

Conclusion

ZnO nanowires with both good crystallinity and oxygen vacancies defects have been synthesized by thermal oxidation of Zn substrate pretreated in concentrated sulfuric acid under the air atmosphere and mixed gas stream (Ar and air), respectively. The PL spectra reveal that only NBE emission peak was observed for the sample grown in the air atmosphere because of its good crystallinity, while the blue–green emission peak was ascribed to oxygen vacancies and their size-dependent Einstein shift was due to bound exciton emission for the samples grown in the mixed gas stream. The HRTEM results and structural simulation confirm that the oxygen vacancies exist in the crystal of the nanowires grown in the mixed gas stream. Therefore, the difference in the above PL spectra is determined by the oxygen vacancies defects in the crystal of ZnO nanowires and their optical properties can be modulated by controlling their crystal structure. The ZnO nanowires grown in the mixed gas stream exhibit better photocatalytic activity than the ZnO nanowires grown in air atmosphere due to the abundant oxygen vacancies too. The photocatalytic degradation of MO obeys the rules of the first-order kinetic reaction and the rate constants were calculated.

Acknowledgments This work was supported by the National Foundations of China–Australia Special Fund for Scientific and Technological Cooperation (grant nos. 20711120186), the Natural Science Foundations of China (grant nos. 20873184), the Natural Science Foundations of Guangdong Province (grant nos. 8151027501000095), and the Science and Technology plan Projects

of Guangdong Province (grant nos. 2008B010600040). The authors would like to thank Professor Hong Liu at School of Chemistry and Chemical Engineering of Sun Yat-sen University.

References

1. G. Kwak, K. Yong, J. Phys. Chem. C **112**, 3036 (2008)
2. T.F. Long, S. Yin, K. Takabatake, P.L. Zhang, Nanoscale Res. Lett. **4**, 247 (2009)
3. H. Wang, Z.P. Zhang, X.N. Wang, Q. Mo, Y. Wang, J.H. Zhu, H.B. Wang, F.J. Yang, Y. Jiang, Nanoscale Res. Lett. **3**, 309 (2008)
4. A. Umar, S.H. Kim, E.K. Suh, Y.B. Hahn, Chem. Phys. Lett. **440**, 110 (2007)
5. J. Zhang, S.R. Wang, M.J. Xu, Y. Wang, B.L. Zhu, S.M. Zhang, W.P. Huang, S.H. Wu, Cryst. Growth Des. **8**, 265 (2008)
6. Y. Wu, Z.H. Xi, G.M. Zhang, J.L. Zhang, D.Z. Guo, Cryst. Growth Des. **8**, 2646 (2008)
7. A. Umar, M.M. Rahman, S.H. Kim, Y.B. Hahn, Chem. Commun. **2**, 166 (2008)
8. Y.C. Liu, Y.H. Tong, J. Nanosci. Nanotechnol. **8**, 1101 (2008)
9. W.D. Chen, P. Wu, X.Q. Zou, J. Appl. Phys. **100**, 054311/1–4 (2006)
10. Z.Q. Chen, S. Yamamoto, M. Makawa, A. Kawasuto, X.L. Yuan, T. Sekiguchi, J. Appl. Phys. **94**, 4807 (2003)
11. T.J. Kuo, C.N. Lin, C.L. Kuo, M.H. Huang, Chem. Mater. **19**, 5143 (2007)
12. A.F. Kohan, G. Ceder, D. Morgan, D.W. Van, G. Chris, Phys. Rev. B: Condens. Matter. **61**, 15019 (2000)
13. D. Li, Y.H. Leung, A.B. Djurisic, Z.T. Liu, M.H. Xie, S.L. Shi, S.J. Xu, W.K. Chan, Appl. Phys. Lett. **85**, 1601 (2004)
14. L. Wischmeier, T. Voss, I. Rueckmann, J. Gutowski, Nanotechnology **19**, 135705 (2008)
15. S. Kar, B.N. Pal, S. Chaudhuri, D. Chakravorty, J. Phys. Chem. B **110**, 4605 (2006)
16. H.M. Hu, X.H. Huang, C.H. Deng, X.Y. Chen, Y.T. Qian, Mater. Chem. Phys. **106**, 58 (2007)
17. Y.L. Yang, H.W. Yan, Z.P. Fu, B.F. Yang, L.S. Xia, Y.D. Xu, J. Zuo, F.Q. Li, Solid State Commun. **138**, 521 (2006)
18. S. Kar, A. Dev, S. Chaudhuri, J. Phys. Chem. B **110**, 17848 (2006)
19. M.C. Jeong, S.W. Lee, J.M. Seo, J.M. Myoung, Nanotechnology **18**, 305701 (2007)
20. R.F. Zhuo, H.T. Feng, J.T. Chen, D. Yan, J.J. Feng, H.J. Li, B.S. Geng, S. Cheng, X.Y. Xu, P.X. Yan, J. Phys. Chem. C **112**, 11767 (2008)
21. A. Umar, Y.B. Hahn, Appl. Surf. Sci. **254**, 3339 (2008)
22. A. Umar, S.H. Kim, J.H. Kim, Y.B. Hahn, J. Nanosci. Nanotechnol. **7**, 4522 (2007)
23. A. Umar, S.H. Kim, J.H. Kim, Y.K. Park, Y.B. Hahn, J. Nanosci. Nanotechnol. **7**, 4421 (2007)
24. M.X. Qiu, Z.Z. Ye, J.G. Lu, H.P. He, J.Y. Huang, L.P. Zhu, B.H. Zhao, Appl. Surf. Sci. **255**, 3972 (2009)
25. J.H. Yang, D.D. Wang, L.L. Yang, Y.J. Zhang, G.Z. Xing, J.H. Lang, H.G. Fan, Y.X. Wang, J. Alloys. Compd. **450**, 508 (2008)
26. X.B. Wang, K.F. Huo, F. Zhang, H. Zheng, P.K. Chu, H.S. Tao, Q. Wu, Y.M. Hu, J.M. Zhu, J. Phys. Chem. C **113**, 170 (2009)
27. H.Q. Liang, L.Z. Pan, Z.J. Liu, Mater. Lett. **62**, 1797 (2008)
28. S. Ren, Y.F. Bai, J. Chen, S.Z. Deng, N.S. Xu, Q.B. Wu, S.H. Yang, Mater. Lett. **61**, 666 (2007)
29. H. Kim, W. Sigmund, Appl. Phys. Lett. **81**, 2085 (2002)
30. H.B. Lu, H. Li, L. Liao, Y. Tian, M. Shuai, J.C. Li, M.F. Hu, Q. Fu, B.P. Zhu, Nanotechnology **19**, 045605 (2008)
31. X.G. Wen, Y.P. Fang, Q. Pang, C.L. Yang, J.N. Wang, W.K. Ge, K.S. Wong, S.H. Yang, J. Phys. Chem. B **109**, 15303 (2005)
32. H.Y. Dang, J. Wang, S.S. Fan, Nanotechnology **14**, 738 (2003)
33. T.W. Kim, T. Kawazoe, S. Yamazaki, M. Ohtsu, T. Sekiguchi, Appl. Phys. Lett. **84**, 3358 (2004)
34. F.L. Deepak, P. Saldanha, S.R.C. Vivekchand, A. Govindaraj, Chem. Phys. Lett. **417**, 535 (2006)
35. H.H. Li, C.L. Liang, M. Liu, K. Zhong, Y.X. Tong, P. Liu, G.A. Hope, Nanoscale Res. Lett. **4**, 47 (2009)
36. U. Ozgur, Y.L. Alivov, C. Liu, A. Teke, M.A. Reshchikov, S. Dogan, V. Aurutin, S.J. Cho, H. Morkoc, J. Appl. Phys. **98**, 041301 (2005)
37. A. Umar, Y.B. Hahn, Cryst. Growth Des. **8**, 2741 (2008)
38. A. Umar, B. Karunagaran, S.H. Kim, E.K. Suh, Y.B. Hahn, Inorg. Chem. **47**, 4088 (2008)
39. A. Umar, S.H. Kim, H. Lee, N. Lee, Y.B. Hahn, J. Phys. D **41**, 065412/1–6 (2008)
40. A. Umar, E.K. Suh, Y.B. Hahn, J. Phys. D **40**, 3478 (2007)
41. Y.W. Heo, D.P. Norton, S.J. Pearton, J. Appl. Phys. **98**, 073502/1–6 (2005)
42. B.X. Lin, Z.X. Lin, Z.X. Fu, Y.B. Jia, Appl. Phys. Lett. **79**, 943 (2001)
43. C.H. Ahn, Y.Y. Kim, D.C. Kim, S.K. Mohanta, C.H. Koun, J. Appl. Phys. **105**, 013502/1–5 (2009)
44. J.H. Li, C.Y. Liu, C.L. Shao, X.T. Zhang, D.Z. Shen, Y.M. Lu, J.Y. Zhang, X.W. Fan, J. Colloid Interface Sci. **283**, 513 (2005)
45. M. Yin, Y. Gu, I.L. Kuskovsky, T. Andelman, Y.M. Zhu, G.F. Neumark, S. O'Brien, J. Am. Chem. Soc. **126**, 6206 (2004)
46. P.D. Yang, H.Q. Yan, S. Mao, R. Russo, J. Johnson, R. Saykally, N. Morris, J. Pham, R.R. He, H.J. Choi, Adv. Funct. Mater. **12**, 323 (2002)
47. J. Zhou, Y. Ding, S.Z. Deng, L. Gong, N.S. Xu, Z.L. Wang, Adv. Mater. **17**, 2107 (2005)